

CIPANP2018-Arrington  
October 23, 2018

# Inclusive Studies of Short-Range Correlations: Overview and New Results

ZHIHONG YE, JOHN ARRINGTON<sup>1</sup>

*Physics Division, Argonne National Lab, Lemont, IL, USA*

We present an overview of Short-Range Correlations (SRC) studies using the inclusive measurement of the electron scattering off nuclei. A brief introduction of the origin of the SRC is given, followed by the survey of the two-nucleon SRC (2N-SRC) study and its interesting connection to the EMC effect. A discussion of the three-nucleon SRC study (3N-SRC) measured by the Jefferson Lab's Hall B and Hall C experiments which showed contradictory results is given and, most importantly, we report a new result from the Hall A E08-014 experiment which was dedicated on studying 3N-SRC. Our high precision  $^4\text{He}/^3\text{He}$  cross section ratios at  $x > 2$  region do not show a 3N-SRC plateau as predicted by the naive SRC model. To further investigate the 3N-SRC as well as the isospin effect of the SRC, we have designed several approved experiments in Hall A and in Hall C, including the Tritium experiments using the mirror nuclei ( $^3\text{H}$  and  $^3\text{He}$ ) which are currently running in Hall A.

PRESENTED AT

CIPANP 2018  
Palm Springs, CA, May 29 - June 3, 2018

---

<sup>1</sup>This work was supported by the U.S. Department of Energy, Office of Science, Office of Nuclear Physics under contract DE-AC02-06CH11357.

# 1 Short-Range Correlations

Nuclei are composed of nucleons, i.e. protons and neutrons, whose interactions are relatively weak at typical inter-nucleon distances ( $>2$  fm), but much stronger at short distances ( $\sim 1$  fm). At small separation, the nucleons' two-body potential, dominated by tensor force, becomes much stronger until their hard cores start to push nucleons away from each other, resulting in strong repulsive force, shown in Fig. 1. Mean-Field theory, such as the Shell-Model, has been a successful theory to describe how nucleons move inside a nucleus below the typical Fermi-momentum ( $k_F \approx 250$  MeV/c). There is, however, still significant contribution from nucleons that carry momentum above the Fermi-motion, indicated by the high momentum tail of a nucleon's momentum distribution in a nucleus [1]. Even in  $^2\text{H}$ , nearly half of its kinematic energy comes from the 5% of nucleons with momentum above the Fermi-momentum. These fast-moving nucleons come mainly from the strong short-range interactions associated with the tensor force and hard repulsive core of the nucleon-nucleon interaction. As such, these high-momentum nucleons correspond to highly localized configurations, referred to as Short-Range Correlations (SRC). While the mean field parts of the momentum distributions reveal strong  $A$ -dependence, the consequence of SRC is the  $A$ -independent high momentum tails at  $k > k_F$  in different nuclei, as shown in Fig. 2.

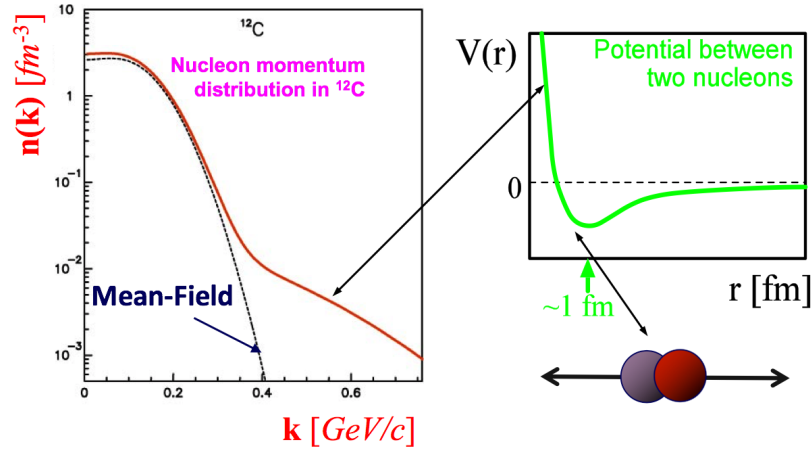


Figure 1: Momentum distribution for carbon in the Mean-Field approach and explicitly including the short-range two-body nucleon interactions. Figure adopted from Ref. [1]

One can perform  $A(e, e'p)$  experiments and, in a plane-wave interpretation, extract the momentum distribution of protons in the nucleus. The contribution of SRCs is isolated by looking for the high-momentum nucleons in the initial state generated by the short-range configurations, which appear at high missing momentum. However,

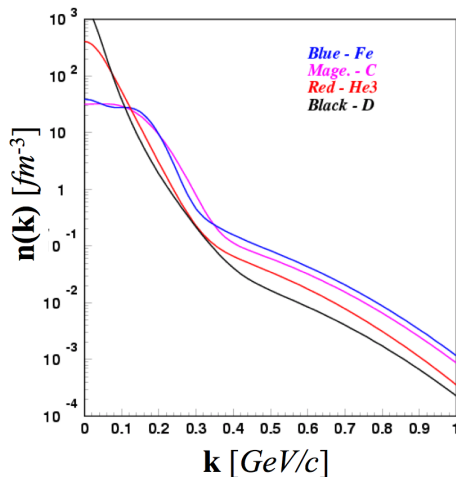


Figure 2: Momentum distributions among light to heavy nuclei.

such measurements also include contributions from final-state interactions (FSIs), meson-exchange currents (MEC), and isobar contributions (IC). Even for measurements at large  $Q^2$  values, the FSI contribution tend to be significant for measurements at large missing momentum [2, 3]. This makes it extremely difficult to isolate the contribution from SRCs. Despite the limitations of  $A(e,e'p)$  measurements, they have been successfully used to identify scattering events which appear to come from high-momentum protons in the initial state, allowing a direct test of the SRC picture by looking for the partner nucleon from the SRC with momenta opposite of the struck nucleon [4, 5]. These data support the SRC model, and also demonstrated that np pairs dominate the high-momentum component of the nuclear momentum distribution.

In inclusive scattering, these final state interactions are significantly suppressed. However, one cannot directly reconstruct the initial momentum of the struck nucleon. Despite this, one can still isolate SRC contributions by measuring the inclusive cross sections in select kinematic regions, e.g. large  $Q^2$  and  $x > 1.4 - 1.5$ . For these kinematics, FSI and MEC effects and inelastic contributions are largely suppressed, and at large  $x$ , the scattering is sensitive only to scattering from nucleons above a minimum momentum which can be selected to isolate SRCs by choosing appropriate  $Q^2$  and  $x$  values, as shown in Fig. 3. This allows us to isolate SRC contributions and compare their strength and structure in different nuclei. Thus, we can examine the relative contribution of SRCs in different nuclei and verify their universal character, but we do not have enough information to reconstruct the initial momentum of the knock-out protons, nor to directly observe the back-to-back motion of the nucleon pairs in the center of mass frame.

The inclusive QE cross section of electron scattering off a nucleus ( $A$ ) at  $x > 1$  can

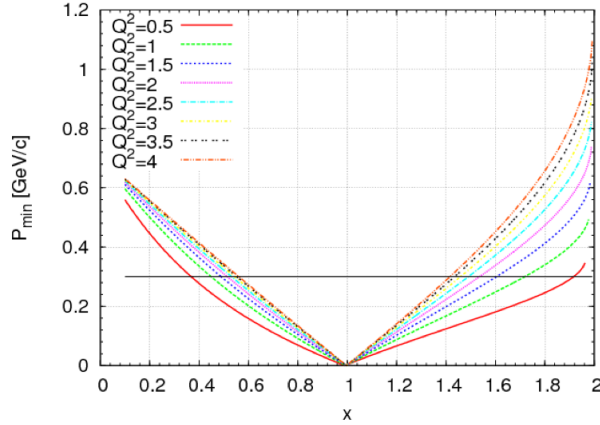


Figure 3: Correlation of  $Q^2$  and  $x$  corresponding to different nucleon initial momenta. Figure from Ref. [6]

be decomposed into contribution from single-particle states, two-body, three-body, and N-body contributions, in the simple SRC model [7], neglecting center-of-mass motion of the N-body configurations, as

$$\sigma_{QE}^A(x) = \sigma_{MF}^A(x) + a_2\sigma_2^A(x) + a_3\sigma_3^A(x) + \dots, \quad (1)$$

where  $\sigma_{MF}^A(x)$  denotes the contribution from the mean-field part, while  $\sigma_2^A(x)$  ( $\sigma_3^A(x)$ ) represents the contribution from the 2N-SRC (3N-SRC).  $a_2^A$  ( $a_3^A$ ) gives the probability of forming the 2N-SRC (3N-SRC) configuration and should show the scaling behavior in the range of  $1 < x < 2$  ( $2 < x < 3$ ).

If kinematics are selected such that scattering requires initial momenta above the Fermi momentum, then the mean-field contribution is negligible and the cross section reduces to

$$\sigma_{QE}^A(x) = a_2\sigma_2^A(x) + a_3\sigma_3^A(x) + \dots. \quad (2)$$

This is typically achieved by requiring  $Q^2 \gtrsim 1-2 \text{ GeV}^2$  and  $x > 1.4-1.5$ . With 3N-SRC contributions expected to be small below  $x=2$ , this implies a universal behavior for the cross section in these kinematics, as demonstrated in the QE cross sections of these nuclei, shown in Fig. 4. Near the QE peak, the cross section has a strongly  $A$ -dependent shape, with a narrow, pronounced QE peak for light nuclei, and a washed-out peak for heavier nuclei. However, above  $x \approx 1.4$ , the cross section shows a universal behavior, with only the normalization varying with  $A$ .

This universal behavior is more clearly seen in Fig. 5, where ratios of heavy nuclei to  $^2\text{H}$  and  $^3\text{He}$  are shown from measurements in Halls B and C. The large- $x$  plateau demonstrates the universal behavior of the cross section, and the ratio corresponds to the relative contribution of 2N-SRCs from the heavy nucleus relative to  $^2\text{H}$  or  $^3\text{He}$ .

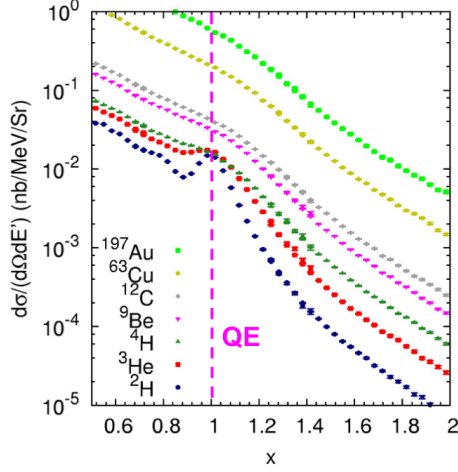


Figure 4: Inclusive quasi-elastic cross section distributions among light to heavy nuclei [8].

Extending this to the region above  $x=2$ , Eq. 1 predicts a similar plateau for  $x > 2$ , allowing the extraction of  $a_2^A$  and  $a_3^A$ :

$$a_2^A = \frac{2}{A} \frac{\sigma_2^A(x)}{\sigma_2^{2H}(x)}, \quad a_3^A = \frac{3}{A} \frac{\sigma_3^A(x)}{\sigma_3^{3He}(x)}. \quad (3)$$

The contribution of 2N-SRCs has been well studied and shows good agreement between the data from SLAC [7] and from Jefferson Lab's Hall B [9] and Hall C [10]. Fig. 5 shows a clear 2N-SRC plateau in both the  $A/{}^3\text{He}$  and  $A/{}^2\text{H}$  ratios for  $1.5 < x < 2$ , despite the different  $Q^2$  ranges and nuclei in the denominator. The scaling plateau in the cross section ratio conforms the similarity of the momentum distributions among nuclei when  $k > k_F$  suggested in Fig. 2, while the plateau values corresponding to  $a_2^A$  gives the probability of a nucleon in a 2N-SRC pair. The value of  $a_2^A$  changes rapidly with  $A$  for light nuclei, but grows slowly for above  $A = 12$ , with heavier nuclei yielding  $a_2 \approx 5$ . For many years after the initial observation of SRCs [7], it was assumed that the contribution of SRCs, measured through the value of  $a_2^A$ , scaled with the nuclear density [9]. This was natural as the typical nucleons separation, and thus the likelihood to interact via the short-range parts of the NN potential, increase with the nuclear density, and was supported by measurements of  $a_2^A$  until the data from Ref. [10]. This data demonstrated showed that  $a_2^A$  for  ${}^9\text{Be}$  deviated significantly from the assumed scaling with the average nuclear density. This was the first observation that details of nuclear structure had a significant impact on the relative contribution from SRCs.

As noted earlier, the JLab E01-015  ${}^{12}\text{C}(e,e'pN)$  experiment demonstrated that np pairs dominate SRCs [4], as a consequence of the dominance of the tensor force in at

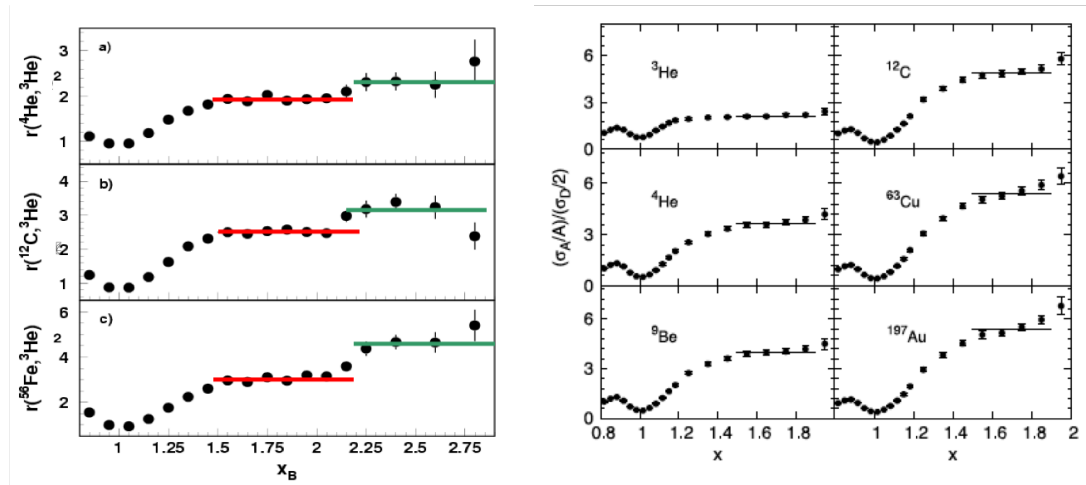


Figure 5: Inclusive cross section ratio of nuclei to  ${}^3\text{He}$  from Hall B CLAS result (left) [9] and nuclei to  ${}^2\text{H}$  from Hall C results (right) [10]

these momenta. While inclusive measurements combine contributions from protons and neutrons, we can still use inclusive scattering to study the isospin structure of SRCs by comparing targets with different isospin structure. The JLab Hall A E08-014 experiment [11] studied Calcium isotope,  ${}^{48}\text{Ca}$  and  ${}^{40}\text{Ca}$ , to test the np-dominance picture in inclusive scattering, where FSI contributions are expected to be much smaller. An ongoing experiment in Hall A, E12-11-112 [12], is measuring the inclusive QE cross section ratio of  ${}^3\text{He}$  to  ${}^3\text{H}$  which is predicted to have much greater sensitivity than measurements using the Calcium isotopes.

## 2 2N-SRC and EMC Effect

The EMC effect was discovered in the 1980s by the European Muon Collaboration at CERN. When using heavy nuclei as effective nucleon target to perform high precision measurement of quark parton distribution functions (PDF), they observed an A-dependent slope in the range of  $0.3 < x < 0.7$  when taking DIS cross section ratio between nucleus A to deuterium [13]. As with the contribution of SRCs, the EMC effect was observed to scale with the average density of the nucleus. The most recent measurement of the EMC effect in Hall C at Jefferson Lab [14] made a more precise measurements of the EMC effect in light nuclei up to  ${}^{12}\text{C}$ . The data showed that the size of the EMC effect does not depend simply on the average nuclear density. The  ${}^9\text{Be}$  EMC effect, as quantified by the slope of the  $A/{}^2\text{H}$  ratios, deviates from the trend observed in other nuclei, as shown in Fig. 6.  ${}^9\text{Be}$  is known to have a configuration of two alpha plus a neutron so the observation suggests that the EMC effect also depends

on the local density. This same behavior was later observed in the measurement of  $a_2^A$ , also shown in Fig. 6.

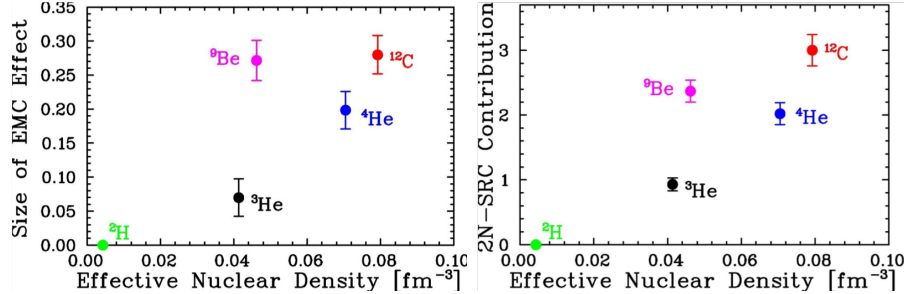


Figure 6: Size of the EMC effect [14] (left) and contribution from SRCs [10] (right) as a function of nuclear density in light nuclei. Figure adopted from Ref. [14].

For light nuclei, these can be examined as a function of density as calculated from *ab initio* calculations [15]. One can include heavy nuclei in the comparison and avoid any model dependence by directly comparing the EMC effect and contribution from SRCs, which shows a clear correlation between these effects, even for <sup>9</sup>Be where both effects deviation from the simple density dependence, as shown in Fig. 7. This has led to the suggestion that both the EMC effect and SRCs depend on the same aspect of nuclear structure, or that one of these is responsible for the other [16]. For example, in the former case, the short-distance configurations can be taken as the cause for both the SRCs, which arise from the short-distance interactions, and the EMC effect if it is connected to the local high-density configuration associated with two overlapping nucleons. For the latter case, it is sometimes assumed that the EMC effect comes from off-shell effects associated with high-momentum nucleons, and thus that high-momtenta associated with SRCs is the direct cause of the EMC effect. Existing data do not provide enough information to separate these (or other) explanations [16], although such pictures do make different predictions about other observables, e.g. the flavor-dependence of the EMC effect [17].

### 3 3N-SRC and New Results

Unlike the 2N-SRC contributions, 3N-SRC contributions have not been clearly identified, and the CLAS data in Hall B and the E02-019 data in Hall C results didn't show agreement in the  $x > 2$  region [10]. As shown in Fig. 5, the CLAS result show clear plateaus for  $A/{}^3\text{He}$  cross section ratios for  $x > 2.25$  for three different nuclei. The E02-019 result, taken at larger  $Q^2$  values (roughly 2.8 GeV<sup>2</sup>, as opposed to  $\sim 1.6$  GeV<sup>2</sup> for the CLAS data) have larger uncertainties but show significantly larger ratios in the  ${}^4\text{He}/{}^3\text{He}$  ratios for  $x > 2.3$ . This suggests an inconsistency between the data sets

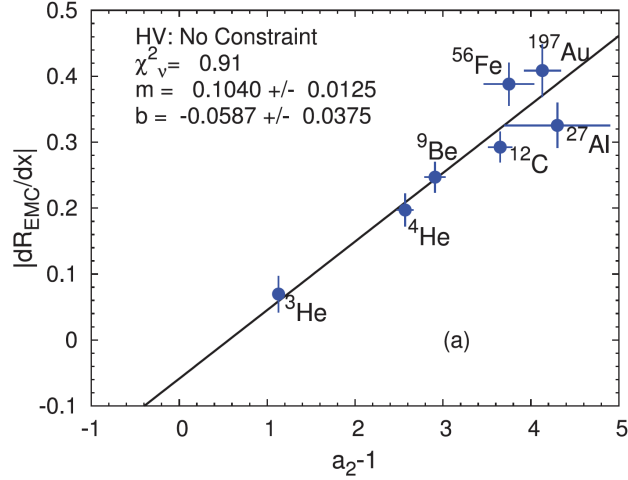


Figure 7: The linear correlation between the SRC and the EMC effect. Figure is from [16].

or else an unexpectedly large  $Q^2$  dependence in the ratios. One possible explanation of the discrepancy was presented in Ref. [19], suggesting that due to its limited momentum resolution, the CLAS result has large bin migration effects at large  $x$  where the cross section drops rapidly for  $^3\text{He}$ .

Experiment E08-014 [11] in Hall A performed a dedicated measurement of the  $x$  and  $Q^2$  dependence of the ratio at  $x > 2$  with the high-resolution spectrometers for  $Q^2$  values close to the CLAS data. The result [18] is consistent in the 2N-SRC region with the CLAS and E02-019 results, as shown in Fig. 8. However, the much higher precision result at  $x > 2$  shows no indication of the 3N-SRC plateau seen in the CLAS data. This rules out the idea of a large  $Q^2$  dependence in the ratio, and is consistent with the explanation presented in [19]. These results show that there is no plateau in the  $^4\text{He}/^3\text{He}$  in the 3N-SRC region at these  $Q^2$ , but does not rule out the presence of significant 3N-SRC contributions. While the prediction for plateaus in the 2N-SRC region is robust, it is much more difficult to predict where such a plateau should be seen for 3N-SRCs, or even if it will present itself in this fashion [18].

This leaves us with the question of whether or not 3N-SRC are important in nuclei, and demonstrates the need for further theoretical and experimental work to provide a clear and quantitative statement on their contributions in nuclei. Isolating 2N-SRC requires  $x > 1.4$  and  $Q^2 \geq 1.5 \text{ GeV}^2$ . At  $x \rightarrow 2$  the scaling behavior of the 2N-SRC breaks down due to the strong motion of the 2N-SRC pair in a nucleus. When  $x$  gets even larger, one expects that the 2N-SRC contribution is eventually overwhelmed by the 3N-SRC contributions. However, it is not clear when this transition happens. Some theoretical calculations, e.g. [20], argue that a much larger  $Q^2$  is needed to ( $Q^2 > 10 \text{ GeV}^2$ ) to be sensitive to the 3N-SRC for  $x > 2$ . At the E08-014 kinematic



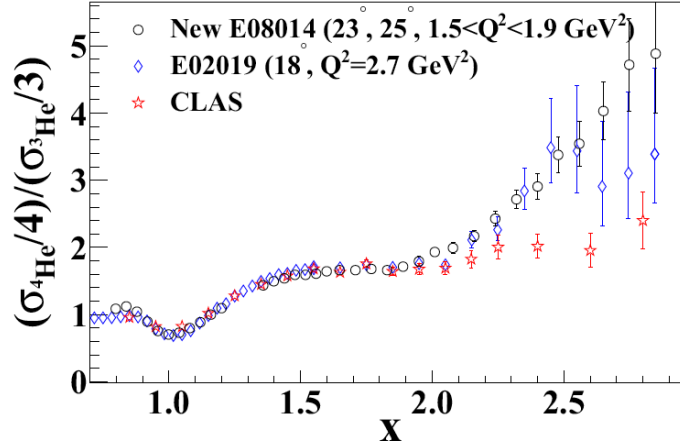


Figure 8: New  ${}^4\text{He}/{}^3\text{He}$  cross section ratio result from the Hall A E08-014 experiment [18]

region, the ratio has strong  $Q^2$  dependent as shown in Fig. 9, and the onset of the 3N-SRC may show up very late, e.g.  $x > 2.5$ . On the other hand, one should also note that unlike the 2N-SRC pair which always contains two back-to-back nucleons, the momentum balance in a 3N-SRC cluster allows for a range of symmetric and asymmetric distributions in terms of both momentum and isospin. Fig. 10 shows the QE cross-section distribution from the E08-014 data up to  $x = 3$  for multiple nuclei. One can clearly see that the distributions indicate scaling behavior in  $1.5 < x < 2$  which gives the 2N-SRC plateau. When  $x$  becomes larger, the  ${}^3\text{He}$  drops significantly faster than other nuclei and eventually goes to zero at  $x \rightarrow 3$ . Compared with the deuterium cross sections, one can conclude that the motion of the 3N-SRC has larger effect near  $x = 3$  which possibly cause the onset of the 3N-SRC deforms much earlier before  $x \rightarrow 3$ .

## 4 Summary and Future Perspective

In the last three decades, lots of progress have been made in term of studying the nucleon-nucleon interaction in a dramatic form where the SRC describe the feature when nucleons are largely overlapped. Many interesting results were released from experiments at SLAC, BNL, and JLab. During the JLab 12GeV era, we have a set up of new experiments that have been approved to continue pursue the topic of SRC using inclusive scattering and systematic study the connection between the SRC and the EMC effect. The Hall A Tritium run group experiments, which have been running from December 2017 to the end of 2018, will explore the isospin effect in SRC and 3N-SRC using the inclusive QE scattering off  ${}^3\text{He}$  and  ${}^3\text{H}$  [12], and also study the

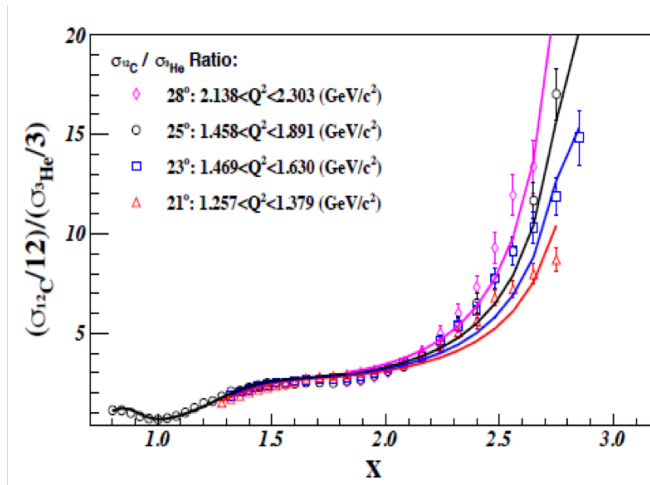


Figure 9: The  $^4\text{He}/^3\text{He}$  ratios at different  $Q^2$  from the E08-014 data [18]

EMC effect using deep inelastic scattering off these two nuclei [21]. In Hall C, multiple experiments were carefully designed to investigate the SRC and the EMC effects in a much broader kinematic region with a very similar set of nuclear targets [22, 23].

## ACKNOWLEDGEMENTS

This work was supported by the U.S. Department of Energy, Office of Science, Office of Nuclear Physics, under contract DC-AC02-06CH11357.

## References

- [1] C. Degli Atti, *et. al.*, Phys. Rev. C53 (1996) 1689
- [2] M. M. Sargsian, *et. al.*, J.Phys. G29 (2003) R1
- [3] J. Arrington, D. Higinbotham, G. Rosner, M. Sargsian, Prog.Part.Nucl.Phys. 67 (2012) 898
- [4] R. Subedi *et. al.*, Science 320, 1476 (2008)
- [5] I. Korover, *et. al.*, Phys. Rev. Lett. 113 (2014) 022501
- [6] N. Fomin, D. Higinbotham, M. Sargsian and P. Solvignon, Ann. Rev. Nucl. Part. Sci. **67**, 129 (2017)

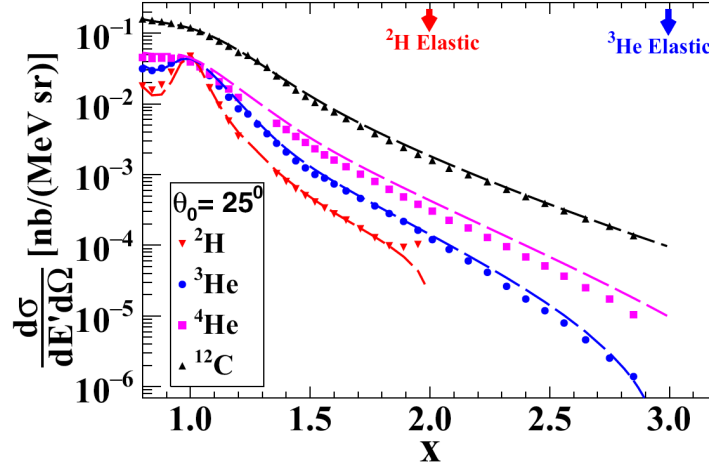


Figure 10: New QE cross section results for multiple nuclei from the Hall A E08-014 experiment [18]

- [7] L. Frankfurt , M. Strikman, D. B. Day, M. Sargsyan, Phys. Rev. C 48 (1993) 2451
- [8] N. Fomin, Ph.D Thesis, University of Virginia
- [9] K. Egiyan, *et. al.*, Phys. Rev. Lett. 96 (2006) 082501
- [10] N. Fomin, *et. al.*, Phys. Rev. Lett. 108 (2012) 092052
- [11] *E08-014: SRC at  $x > 2$*  , Approved Hall A 6 GeV Experiment at Jefferson Lab, J. Arrington, D. Day, D. Higinbotham, P. Solvignon
- [12] *E12-11-112: SRC and Isospin Effect using  $^3H$  and  $^3He$  at 12GeV*, Approved Hall A Experiment at Jefferson Lab, J. Arrington, D. Day, D. Higinbotham, P. Solvignon
- [13] J. Aubert, *et. al.*, Phys. Lett. B 123 (1983) 275
- [14] J. Seely, *et. al.*, Phys. Rev. Lett. (2009) 202301
- [15] R.B. Wiringa, R. Schiavilla, S.C. Pieper, J. Carlson, Phys. ReV. C89 (2014) 024305
- [16] J. Arrington, A. Daniel, D. Day, N. Fomin, D. Gaskell, P. Solvignon, Phys. Rev. C86 (2012) 065204
- [17] J. Arrington, EPJ Web Conf. **113**, 01011 (2016)

- [18] Z. Ye, *et. al.*, Phys. Rev. C97 (2018) 065204
- [19] D. Higinbotham and O. Hen, Phys. Rev. Lett., 114 (2015) 169201
- [20] M. Sargsian, Phys. Rev. C 89 (2014) 034305
- [21] *E12-10-103 (MARATHON):  $d(x)/u(x)$  and EMC Effect using  $^3H$  and  $^3He$  at 12GeV*, Approved Hall A Experiment at Jefferson Lab
- [22] *E12-06-105: SRC at  $x > 1$  at 12GeV*, Approved Hall C Experiment at Jefferson Lab, J. Arrington, D. Day, N. Fomin, P. Solvignon
- [23] *E12-10-108: EMC Effect at 12GeV*, Approved Hall C Experiment at Jefferson Lab, J. Arrington, A. Daniel, D. Gaskell,